International Journal of Applied Sciences: Current and Future Research Trends (IJASCFRT)
ISSN: 2790-3990
https://ijascfrtjournal.isrra.org/index.php/Applied_Sciences_Journal

Reynolds Number and Drag Influences on Large Horizontal Axis Wind Turbine Design

Imane Echjijem[a*], Abdelouahed Djebli[b], Mfedel Akdi[c]

[a,b,c]*Energetic Laboratory, Sciences Faculty, Abdelmalek Essaadi University, Tetouan, BP: 2121, Tetouan 93030, Morocco*

[a]*Email: imaneechjijem@gmail.com,* [b]*Email: djebli_abdelouahed@yahoo.fr,* [c]*Email: akdi.m_ffedal-etu@uae.ac.ma*

Abstract

The aerodynamic design of large wind turbines involves many factors, the most important of which are Reynolds number, drag and air density. This paper discusses the influence of these factors on the aerodynamic performance of a large horizontal axis wind turbine covering the drag term in the theoretical analysis. The drag term complicates the system of resolution for the axial and tangential induction factors. Previous work (Mingwei Ge) simplified this system by taking approximations for the axial and tangential induction factors. To make the analysis more general, the nonlinear equation system with the axial and tangential induction factors is solved. In the first step, the effect of Reynolds number Re is studied for the DU00-W-350 blade profile though three values $Re = 2 \times 10^6$, $Re = 6 \times 10^6$, $Re = 10^7$ .Increasing the Reynolds number improves both the torque in the outer section of the blade and the power coefficient along the blade. In the next step, the effect of drag is examined using a comparison between the blade without drag and the blade with drag for the DU00-W-350 and NACA64618 profiles. It is found that a blade profile with lower drag gives higher torque and power coefficient than a blade profile with higher drag. In addition, the air density affects the torque and power coefficient of the NACA64618 blade profile. The simulation of this work is compared to previous work in the literature.

Keywords: Reynolds number; Drag; Air density; Aerodynamic performance.

1. Introduction

Aerodynamic optimization plays a very important role in the development of modern large MW wind turbines, where the overall objective is to increase the power coefficient [1, 2].

Received: 6/5/2023
Accepted: 7/10/2023
Published: 7/25/2023

---

* Corresponding author.

Many researchers are trying to find methods to optimize blade design. Benini and Toffolo presented a bi-objective optimization method to maximize the annual energy production and minimize the energy cost for the design of a horizontal axis wind turbine. A multi-objective evolutionary algorithm and an aerodynamic model based on blade element theory were used to achieve this goal[3].Fuglsang and Madsen aimed to minimize the cost of energy with multiple constraints using a multidisciplinary optimization method for the design of horizontal axis wind turbines. To illustrate the design method, a 1.5 MW stall-regulated rotor was used[4]. Wang and colleagues used Blade Element Momentum (BEM) theory and aerodynamic code to optimize the design of three wind turbine blades at different sizes. The results show that the 2 MW and 5 MW wind turbines can reduce the energy cost of the original rotors more than that of 25 kW wind turbine [1]. Also, in response to the growing demand for large wind turbines, the world has seen significant commercial activity, mainly based on the design of the following wind turbines: Repower 5 MW wind turbines, Siemens 6 MW wind turbines and Vestas 8 MW wind turbines (V164)[5, 6]. The increase in the size of the wind turbine is proportional to the increase in the Reynolds number. In addition, the Reynolds number varies with the air density. For example, for

a 3MW wind turbine blade, the Reynolds number is about for an air density of ,while it is about for an air density of [7].

The Reynolds number has a significant impact on the aerodynamic characteristics of the airfoils such as the lift coefficient C_l ,the drag coefficient C_d and the lift to drag ratio C_l/C_d . Analysis codes like XFOIL and RFOIL present an efficient way to determine the aerodynamic characteristics of airfoils. The design of most aerodynamic profiles of wind turbines at low Reynolds number has been done using the XFOIL code developed by Drela [8, 9]. But at high angles of attack over stall, the XFOIL code does not agree well with wind tunnel tests. Therefore, a modification of XFOIL is necessary to develop a version called RFOIL.Figure1shows a comparison between the XFOIL, RFOIL codes and the experimental results[10].Timmer and Van Rooij (2003) noted that although the RFOIL code does not exactly match the experimental measurements, it can follow the experimental lift curve well after the stall. Researchers Ceyhan[11] and Ge and colleagues [7]were able to study the effects of Reynolds numbers on the aerodynamic characteristics of airfoils and their influence on the optimal shape of a wind turbine blade based on the RFOIL code. Their objective was to maximize the power coefficient. This paper discusses the influence of Reynolds number, drag, and air density on the aerodynamic performance of a large horizontal axis wind turbine covering the drag term in the theoretical analysis. The drag term complicates the system of resolution for the axial and tangential induction factors. Previous work simplified this system by taking approximations for the axial and tangential induction factors. To make the analysis more general, the nonlinear equation system with the axial and tangential induction factors is solved. In the first step, the effect of Reynolds number Re is studied for the DU00-W-350 blade profile though three values: $Re = 2 \times 10^6$, $Re = 6 \times 10^6$, $Re = 10^7$. In the next step, the effect of drag is examined using a comparison between the blade without drag and the blade with drag for the DU00-W-350 and NACA64618 profiles. The effect of air density for the NACA64618 blade profile is also studied. The simulation results are presented in section 3.

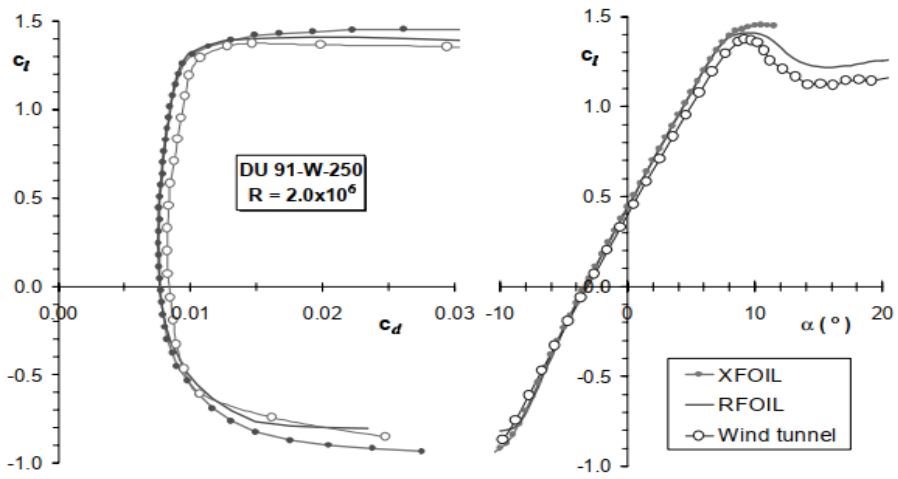

Figure 1: Comparison between codes XFOIL, RFOIL and measurements for DU 91-W2-250 [10].

2. Numerical method

BEM theory is one of the most widely used methods in wind turbine aerodynamics, or rather is a basic method for aerodynamic analysis [12, 13]. Burton and colleagues established a mathematical model based on the BEM theory that maximizes the optimal power coefficient without covering the influence of drag[14]. To account for the drag effect, this part is interested in giving the BEM equations based on the drag factor. The thrust dT and the torque dM given by blade element theory are as follow [7, 14]:

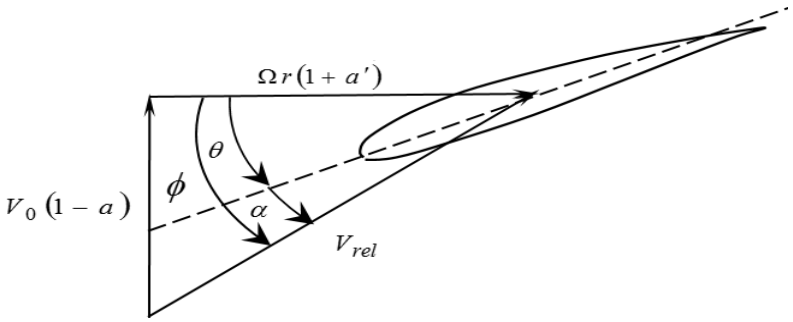

Figure 2: Model of a blade element.

$$dT = \frac{1}{2}\rho N V_{rel}^2 c(r)(C_l \cos\phi + C_d \sin\phi)dr \quad (1)$$

$$dM = \frac{1}{2}\rho N V_{rel}^2 r\, c(r)(C_l \sin\phi - C_d \cos\phi)dr \quad (2)$$

where N is the number of blades, ρ is the air density, C_l and C_d are the lift and drag coefficients respectively, $c(r)$ is the chord length, V_{rel} is the relative wind, ϕ is the inflow angle, θ is the pitch angle. As shown in Figure

2 the velocity triangle gives the following equations:

$$V_{rel} = V_0\sqrt{(1-a)^2 + \lambda^2\mu^2(1+a')^2} \tag{3}$$

$$\phi = \arctan\frac{(1-a)}{\lambda\mu(1+a')} \tag{4}$$

$$\phi = \theta + \alpha \tag{5}$$

where V_0 is the wind velocity, Ω is the angular velocity of rotor, r is the local radius, R is the radius of rotor and $\mu = r/R$, λ is the tip speed ratio, α is the angle of attack which corresponds to the maximum C_l/C_d ratio, a and a' are the axial and the tangential induction factors respectively.

The application of Bernoulli's equation and momentum theory gives the following relations [7][14](see Figure 3):

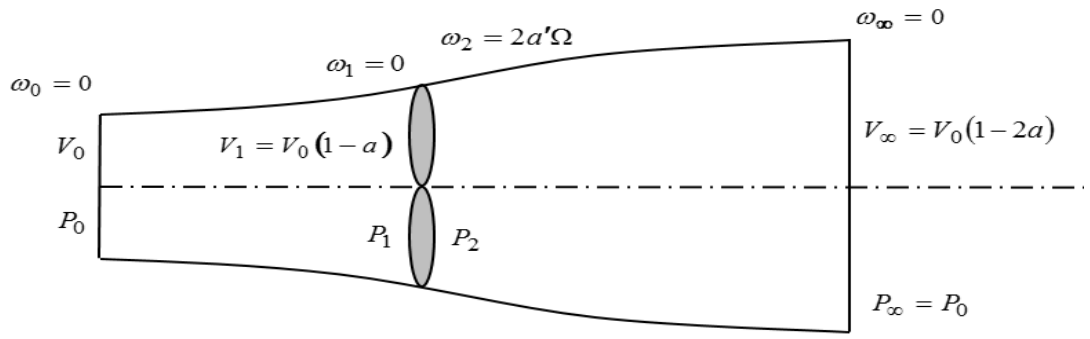

Figure 3: Actuator disc and stream tube of a wind turbine.

$$p_0 + 1/2\rho V_0^2 = p_1 + 1/2\rho V_0^2(1-a)^2 \tag{6}$$

$$p_2 + 1/2\rho V_0^2(1-a)^2 + 1/2\rho(2a'\Omega r)^2 = p_0 + 1/2\rho V_0^2(1-2a)^2 \tag{7}$$

$$p_1 - p_2 = 1/2\rho V_0^2 + 1/2\rho(2a'\Omega r)^2 - 1/2\rho V_0^2(1-2a)^2 \tag{8}$$

where V_i is the axial air velocity at section i, ω_i is the rotational air velocity at section i, p_i is the air pressure at section i .knowing that the thrust equals:

$$dT = (p_1 - p_2)dS \tag{9}$$

$$dT = 4\rho\pi r dr V_0^2 \left(a(1-a) + \lambda^2 \mu^2 a'^2\right) \tag{10}$$

where $dS = 2\pi r dr$ .The torque and power coefficient are given by:

$$dQ = 4a'(1-a)\rho V_0 \Omega \pi r^3 dr \tag{11}$$

$$C_P = 8\lambda^2 \int_{\mu 0}^{1} (1-a)a'\mu^3 d\mu \tag{12}$$

$\mu_0 = r_0 / R$. By equating the thrust and torque of two theories, then simplifying:

$$\frac{V_{rel}^2}{V_0^2} N \frac{c(r)}{R}(C_l \cos\phi + C_d \sin\phi) = 8\pi\mu\left(a(1-a) + \lambda^2 \mu^2 a'^2\right) \tag{13}$$

$$\frac{V_{rel}^2}{V_0^2} N \frac{c(r)}{R}(C_l \sin\phi - C_d \cos\phi) = 8\pi\lambda\mu^2 a'(1-a) \tag{14}$$

Dividing equation (13) by equation (14):

$$\frac{C_l \cos\phi + C_d \sin\phi}{C_l \sin\phi - C_d \cos\phi} = \frac{a(1-a) + \lambda^2 \mu^2 a'^2}{\lambda\mu a'(1-a)} \tag{15}$$

$$\frac{1 + \varepsilon \tan\phi}{\tan\phi - \varepsilon} = \frac{a(1-a) + \lambda^2 \mu^2 a'^2}{\lambda\mu a'(1-a)} \tag{16}$$

Substituting equation (4) into equation (16) gives:

$$\frac{1 + \varepsilon \tan\phi}{\tan\phi - \varepsilon} = \frac{\lambda\mu(1+a') + \varepsilon(1-a)}{1 - a - \varepsilon\mu\lambda(1+a')} \tag{17}$$

where $\varepsilon = C_d / C_l$

Equaling equations (16) and (17), and simplifying:

$$(1-a)\left\{a(1-a) - \lambda^2 \mu^2 a'\right\} - \varepsilon\lambda\mu\left\{a'(1-a) + a(1-a) + \lambda^2 \mu^2 a'^2 (1+a')\right\} = 0 \tag{18}$$

taking into account equation which maximizes the power,

$$\frac{da'}{da} = \frac{a'}{1-a} \tag{19}$$

we obtain equation (20):

$$3a^2 - 2(2-\varepsilon\lambda\mu)a + (1-\varepsilon\lambda\mu) + \frac{\varepsilon\lambda^3\mu^3}{1-a}a'^2(2-3a') = 0 \tag{20}$$

From equations (18) and (20), we have a system of nonlinear equations with two variables a and a':

$$\begin{cases} (1-a)\left[a(1-a) - \lambda^2\mu^2 a'\right] - \varepsilon\lambda\mu\left[a'(1-a) + a(1-a) + \lambda^2\mu^2 a'^2(1+a')\right] = 0 \\ \text{and} \\ 3a^2 - 2(2-\varepsilon\lambda\mu)a + (1-\varepsilon\lambda\mu) + \frac{\varepsilon\lambda^3\mu^3}{1-a}a'^2(2-3a') = 0 \end{cases} \tag{21}$$

The expression of the chord can be obtained from equations (14):

$$\frac{c(r)}{R} = \frac{8\pi\mu}{NC_l}\frac{a'}{(1+a')}\frac{\sin\phi}{(\tan\phi - \varepsilon)} \tag{22}$$

2.1. Case without drag

In the particular case without drag; $\varepsilon = 0$, equations (21) reduce to:

$$\begin{cases} a(1-a) - \lambda^2\mu^2 a' = 0 \\ \text{and} \\ 3a^2 - 4a + 1 = 0 \end{cases} \tag{23}$$

where the solution is:

$$\begin{cases} a' = \frac{a(1-a)}{\lambda^2\mu^2} = \frac{2}{9\lambda^2\mu^2} \\ \text{and} \\ a = \frac{1}{3} \end{cases} \tag{24}$$

therefore,

$$C_P = \frac{16}{27}\left(1-\mu_0^2\right) \tag{25}$$

$$\frac{c(r)}{R} = \frac{16\pi\mu}{NC_l}\frac{\cos\phi}{\left(9\lambda^2\mu^2+2\right)} \tag{26}$$

Clearly, this particular case provides a theoretical upper limit of the aerodynamic efficiency of a horizontal axis wind turbine.

2.2. Case of *[7]*

As in [7], If $\varepsilon \cong 10^{-2}$, $a \cong 10^{-1}$, $a' \cong 10^{-2}$ to 10^{-3}, the system (21) reduce to:

$$\begin{cases} a(1-a)-\lambda^2\mu^2 a'-\varepsilon\lambda\mu\, a = 0 \\ \quad and \\ 3a^2-2(2-\varepsilon\lambda\mu)a+(1-\varepsilon\lambda\mu)=0 \end{cases} \tag{27}$$

where the solution is giving by:

$$\begin{cases} a' = \dfrac{a(1-\varepsilon\lambda\mu-a)}{\lambda^2\mu^2} \\ \quad and \\ a = \dfrac{2}{3}-\dfrac{\varepsilon\lambda\mu}{3}-\dfrac{\sqrt{1-\varepsilon\lambda\mu+(\varepsilon\lambda\mu)^2}}{3} \end{cases} \tag{28}$$

$$C_P = 8\int_0^1 a(1-a)^2\mu d\mu - 8\lambda\int_0^1 a(1-a)\varepsilon\mu^2 d\mu \tag{29}$$

we put : $C_{P1} = 8\int_0^1 a(1-a)^2\mu d\mu$ is independent of ε and $C_{P2} = 8\lambda\int_0^1 a(1-a)\varepsilon\mu^2 d\mu$ depends on ε ,therefore: for $\varepsilon = 0$, $a = 1/3$; $C_{P1} = 0.593$ and for $\varepsilon \neq 0$, $C_{P2} \approx 0.57\lambda\varepsilon$. Equation (29) can be written as a linear formula:

$$C_P = 0.593 - 0.57\lambda\varepsilon \tag{30}$$

Wilson and colleagues (1976) found an expression for the power coefficient that takes into account the drag effect and the tip and root losses as follows [15]:

$$C_P = \left(\frac{16}{27}\right)\lambda\left[\lambda + \frac{1.32 + \left(\frac{\lambda - 8}{20}\right)^2}{N^{2/3}}\right]^{-1} - \frac{0.57\lambda^2}{\frac{C_l}{C_d}\left(\lambda + \frac{1}{2N}\right)} \tag{31}$$

Neglecting the tip and root losses i.e. N tends to infinity, equation (31) becomes:

$$C_P = 0.593 - 0.57\lambda\varepsilon \tag{32}$$

It is evident that equation (32) is in good agreement with equation (30).

3. Results and discussion

3.1 Reynolds number effect

To show the effect of Reynolds number on aerodynamic performance, the DU00-W-350 blade profile was selected and three values of Reynolds number were used $Re = 2\times10^6$, $Re = 6\times10^6$, $Re = 10^7$ at a constant tip speed ratio $\lambda = 10$ .Figure 4 shows the thrust and torque distributions versus the blade length for different Reynolds number, which indicates that the thrust is almost constant near the root, then increases slowly up to the value 2.915×10^4 at the blade tip, and that the torque varied linearly along the blade up to the value 1.059×10^5 at $Re = 10^7$ .It is also observed that the thrust is not affected very much by the variation of Reynolds number, whereas the increase of the Reynolds number affects the increase of the torque in the outer part of blade. Figure5 shows that for a constant tip speed ratio, the increase of the Reynolds number allows to improve the power

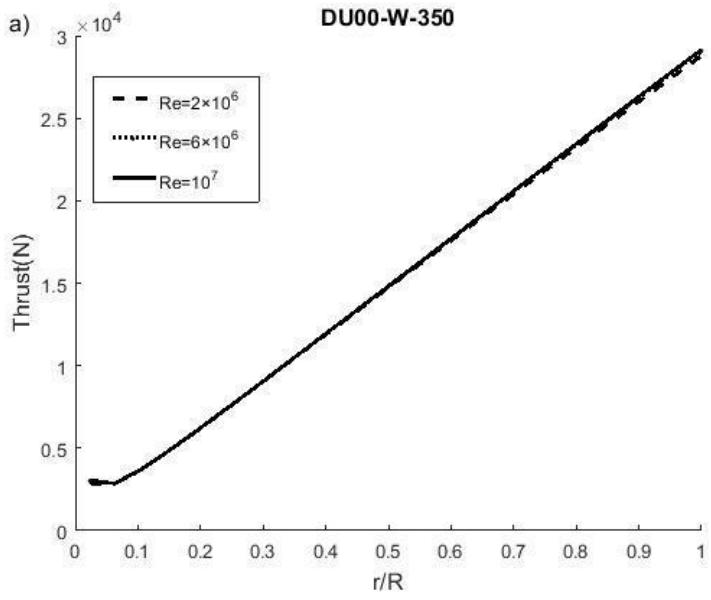

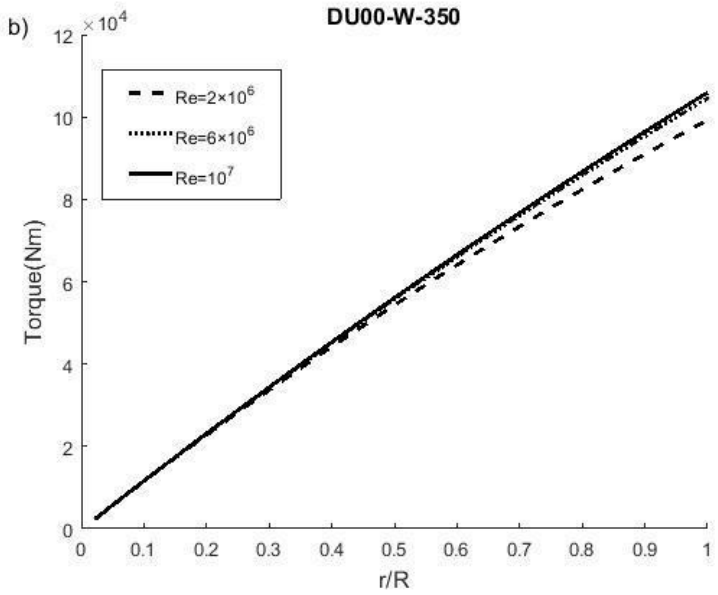

Figure 4: Reynolds number effect on: a) thrust distribution; b) torque distribution.

coefficient along the blade, the rate of improvement of the power coefficient is significant when going from $Re = 2 \times 10^6$ to $Re = 6 \times 10^6$ or to $Re = 10^7$,while this rate is decreased when approaching a high Reynolds number. From $Re = 2 \times 10^6$ to $Re = 10^7$,the amount of increase in terms of maximum power coefficient is 1.12% .

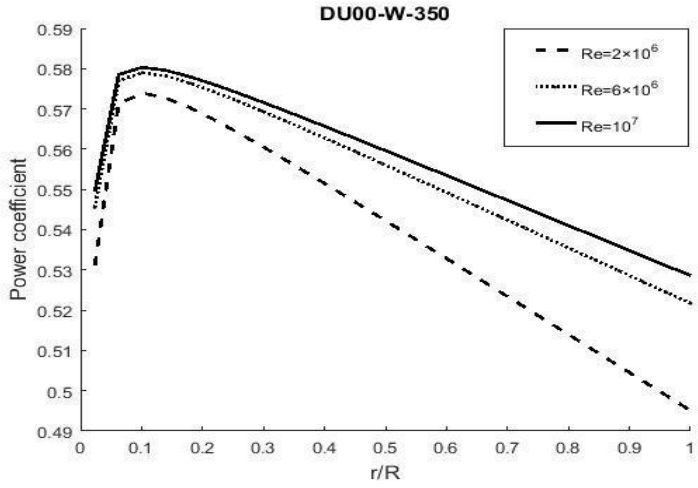

Figure 5: Reynolds number effect on: a) thrust distribution; b) torque distribution.

We adopt Figure 6 which represents the variation of the lift coefficient and drag coefficient as a function of the angle of attack for different Reynolds numbers to give a concrete explanation of the effect of the Reynolds number on the aerodynamic performance. As notices in the figure, the increase of the Reynolds number can increase the lift coefficient and the same time decrease the drag coefficient. Therefore, the increase in aerodynamic performance with Reynolds number is mainly due to the increase in lift coefficient.

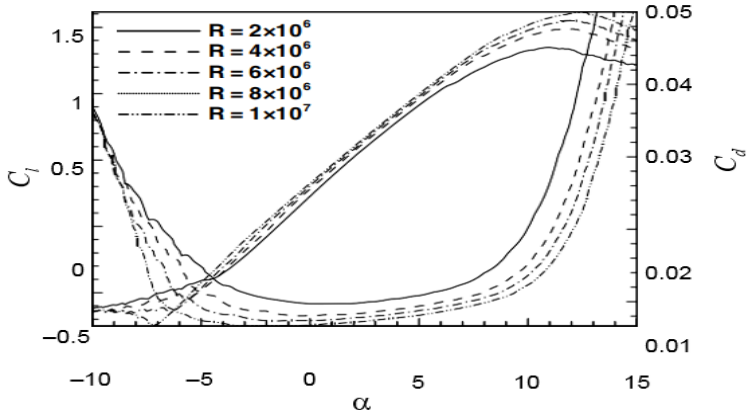

Figure 6: Lift and drag coefficients of DU00-W-350 airfoil at different Reynolds numbers [7].

We see in Figure7 that, at a constant Reynolds number, the low value of tip speed ratio gives higher thrust and torque distributions than the high value of tip speed ratio for all blade positions. It can also be observed in Figure 8 that at a constant Reynolds number, decreasing the tip speed ratio leads to an increase in the power coefficient at positions from $0.1R$ to $1R$,while it leads to a decrease in the power coefficient near the root positions.

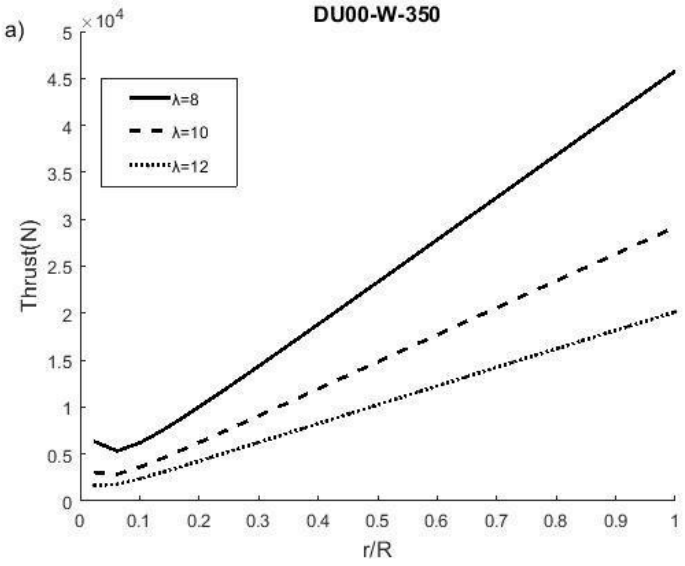

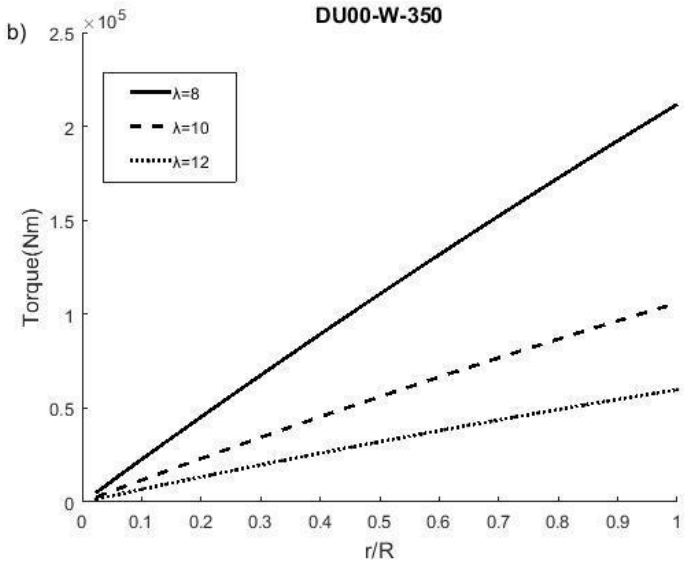

Figure 7: Thrust and torque distributions at different tip speed ratios: a) thrust distribution; b) torque distribution.

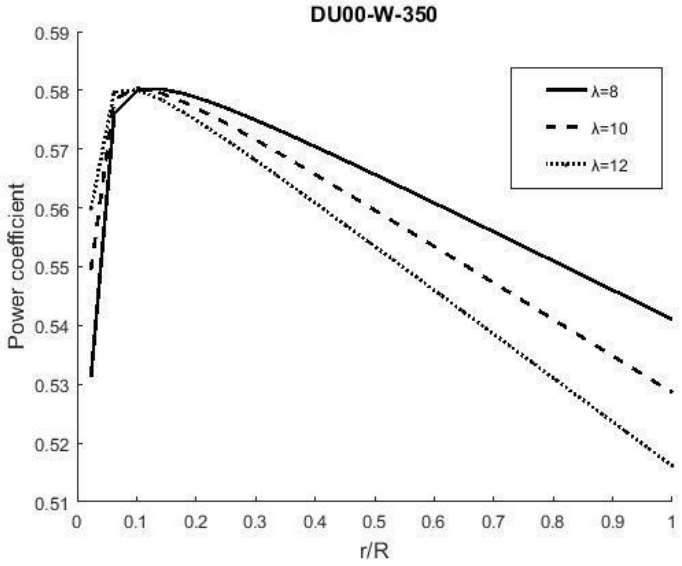

Figure 8: Power coefficient at different tip speed ratios.

3.2. Comparison results

Figure 9 shows comparison results of the axial and tangential induction factors. It shows that the results of the present work agree well with the result of Mingwei Ge for all blade positions. However, the differences are observed near the root positions; For each Re value, it is observed in Figure 9a that near the root of the blade, the axial induction factor of the present work increases until it reaches a maximum value, then it decreases slowly for the rest of the blade. On other hand the axial induction factor of Mingwei Ge begins with a maximum value near the root of the blade, then it decreases slowly for the rest of the blade. For the positions just before the outer part of the blade, the axial induction factor of the present work is higher than that of Mingwei Ge. As

shown in Figure9b, near the root of the blade, the tangential induction factor of the present work is lower than that of Ge.

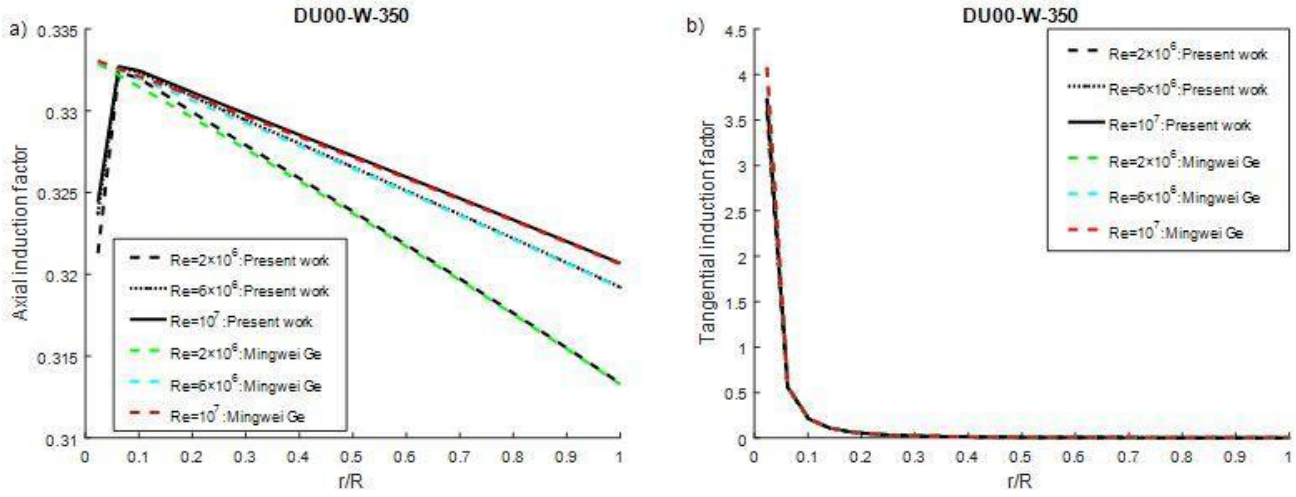

Figure 9: Comparison results of: a) axial induction factor; b) tangential induction factor.

These differences have impacts on the thrust and power coefficient shown in Figure 10a and Figure 11. Figure 10 shows that the results of the thrust and torque distributions are in good agreement with the Mingwei Ge results over the length of the blade, except for the thrust near the root positions which is almost constant for the current work, while it decreases for the Mingwei Ge work. Figure 11 shows that for all Re number values, the power coefficient of the current work is in good agreement with Mingewi's work, while significant differences are recorded near the root where the power coefficient of the current work is lower than Mingwei Ge. In fact, at $Re = 10^7$, the power coefficient of the present work starts with an initial value of 0.5495 , then increases until it reaches a maximum value of 0.5803 . Then, it slowly decreases until it reaches the value 0.5291 . At the same value of Re , Mingewi's power coefficient takes an initial value of 0.5911 , then decreases slowly until it reaches the value 0.5291 .

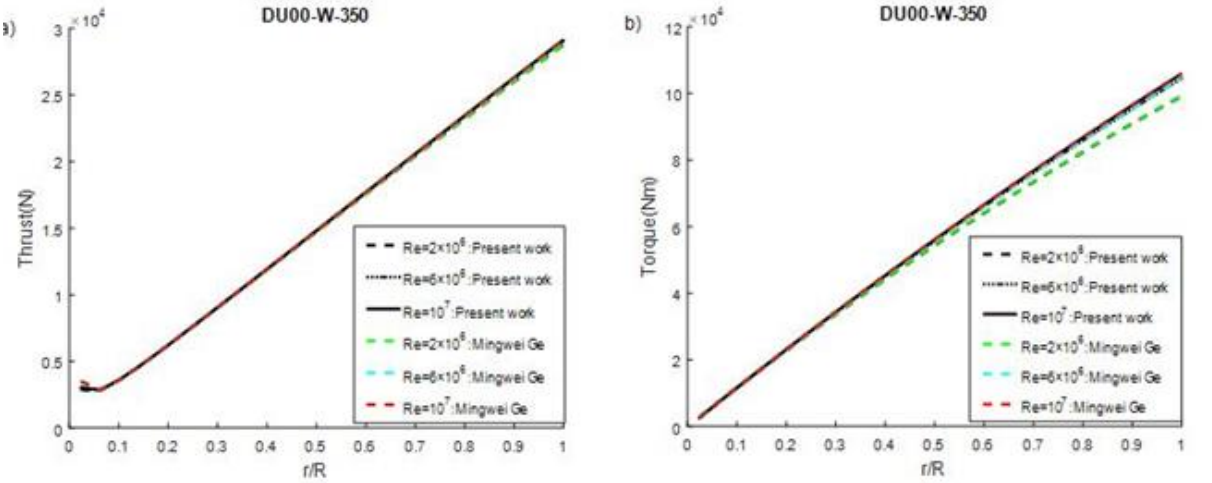

Figure 10: Comparison results of: a) thrust distribution; b) torque distribution.

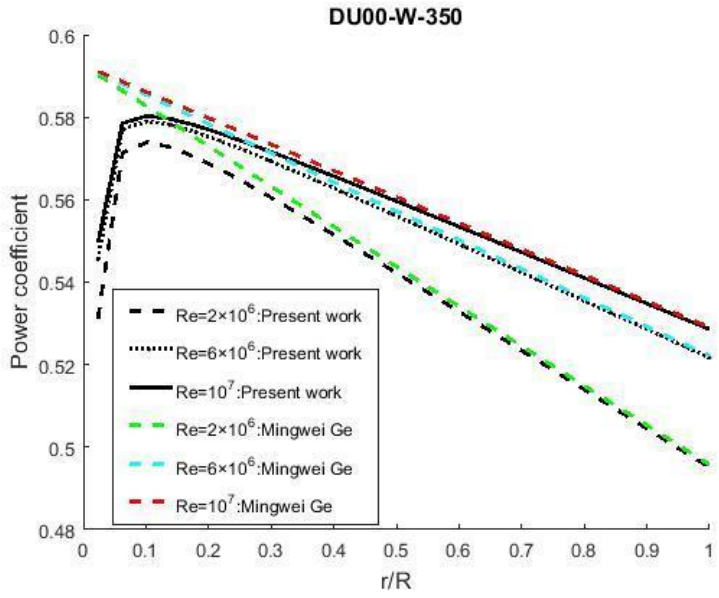

Figure 11: Comparison results of power coefficient.

Figure 12 and Figure 13 show the comparison results of thrust, torque and power coefficient for different values of λ at a constant Re number. For each value of λ, the figures show that the results of current work agree well with the result of Mingwei Ge on blade length. However, the thrust and power coefficient are different from those of Mingwei Ge near the root positions.

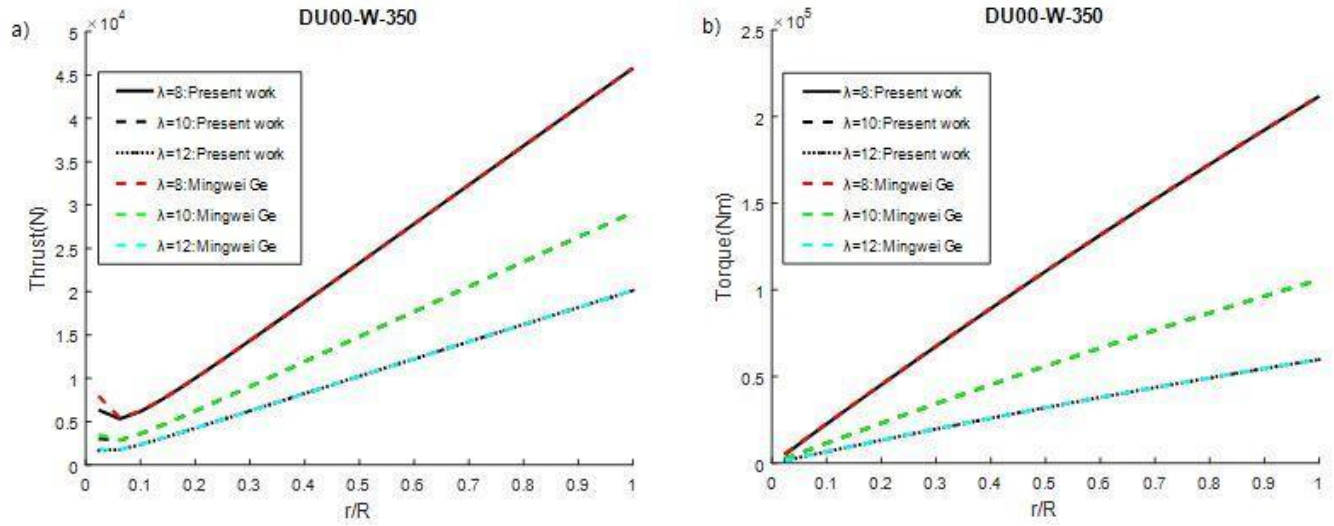

Figure 12: Comparison results of: a) thrust distribution; b) torque distribution.

3.3. Drag effect

At a constants Reynolds number and tip speed ration, a comparison between blade without drag and blade with

drag is examined to evaluate the effect of drag on blade design and aerodynamic performance. The comparison between the chord with and without drag for the NACA64618 and DU00-W-350 blade profiles is given by Figure 14. As shown in the figure, the influence of the chord by the drag is very small and it is recorded

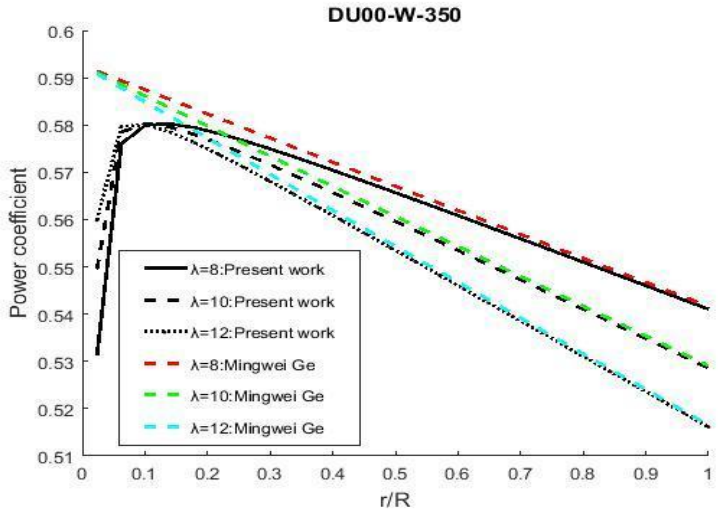

Figure 13: Comparison results of power coefficient at different tip speed ratios.

near the root positions. Moreover, Figure 15 shows that there is no significant difference between twist with and without drag. The thrust distribution with drag is almost similar to that without drag for NACA64618 and DU00-W-350as shown in Figure 16a. However, the torque distribution is influenced by the drag in the outer section of

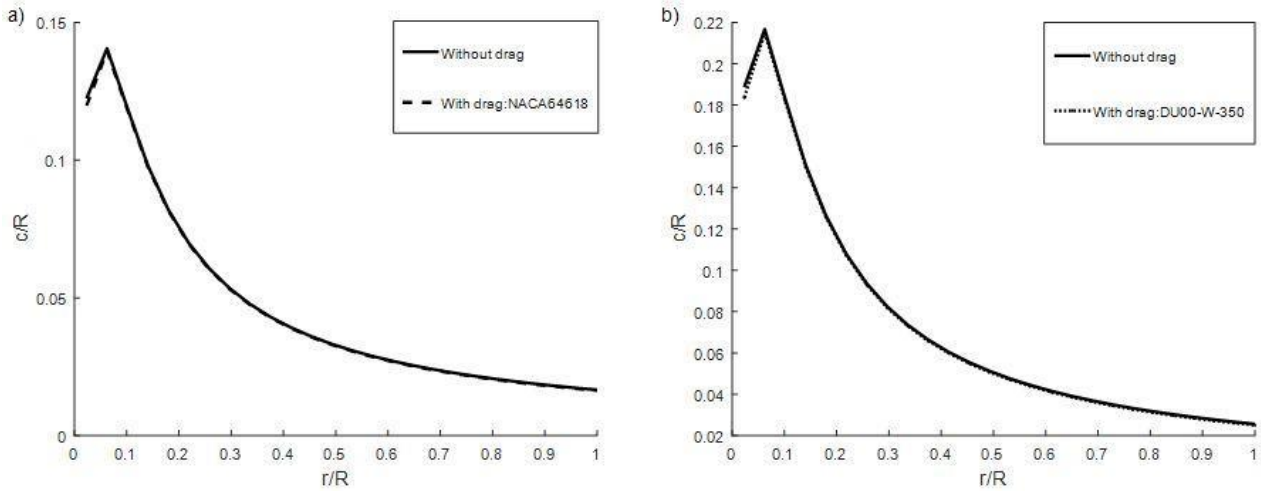

Figure 14: Chord distribution with and without drag for: a) NACA64618; b) DU00-W-350.

the blade, where the torque known a decrease in the presence of the drag than that in absence of the drag for two blade profiles NACA64618 and DU00-W-350, noting that the torque with drag for DU00-W-350 is lower than that of NACA64618.Figure 17 shows that ignoring the drag term, the axial induction factor reaches a theoretical maximum value $a = 1/3$ for all blade positions. However, considering this term, the values of the axial induction

factor are lower than $^{1/3}$ .As shown in Figure 17b, the tangential induction factor with and without the drag term all tend to infinity near the root positions. Figure 18 shows that in the absence of drag, the power coefficient is

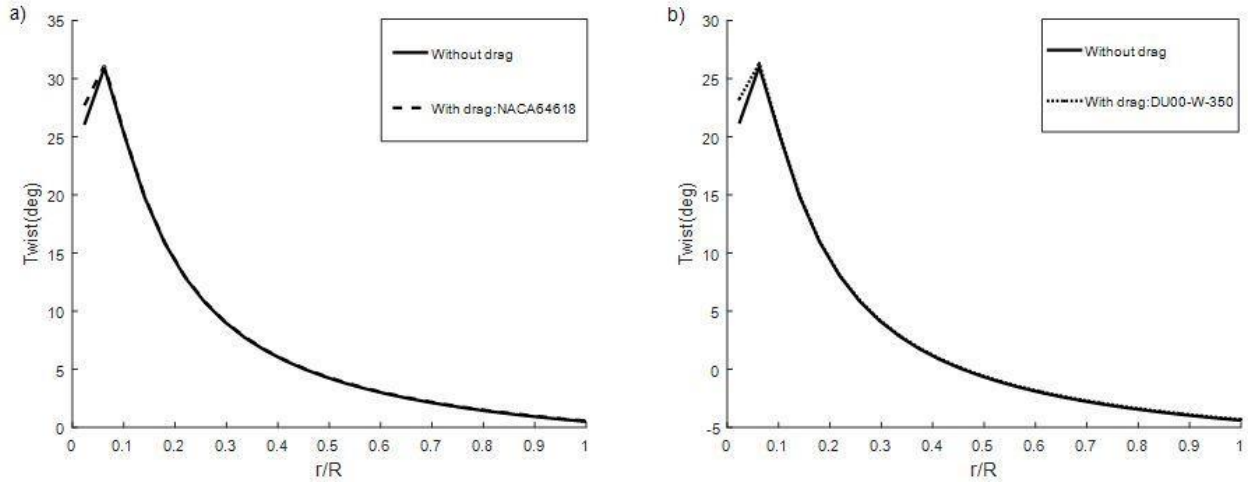

Figure 15: Twist distribution with and without drag for: a) NACA64618; b) DU00-W-350.

uniform along the length of the blade, which is not the case if the drag is involved, where there is clearly a significant reduction in power coefficient. The DU00-W-350 blade profile reduces the power coefficient more than the NACA64618 blade profile.

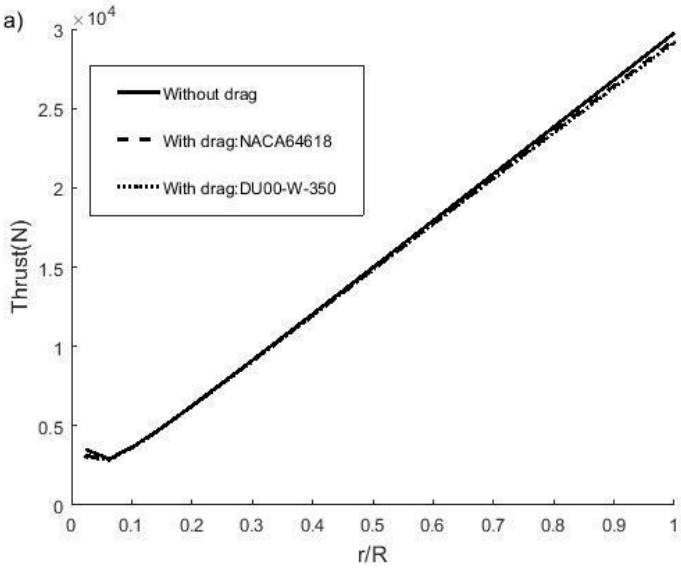

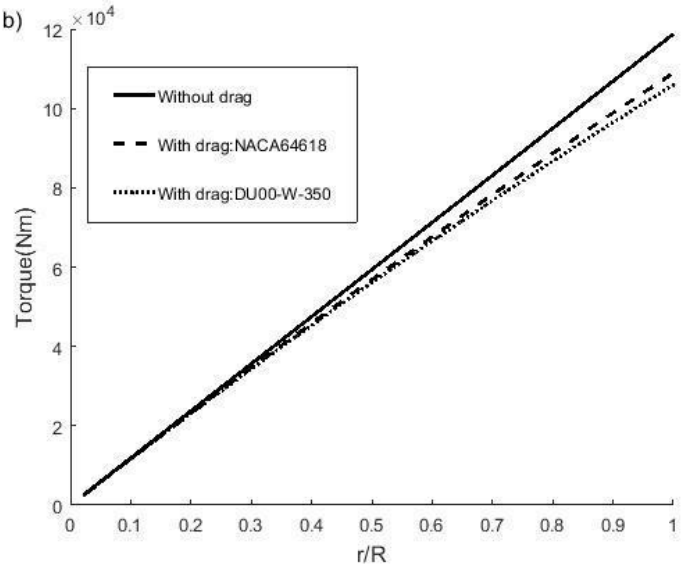

Figure 16: Drag effect on: a) thrust distribution; b) torque distribution

The maximum power coefficient for the blade without drag is 0.5926 and for the blades with drag: NACA64618 and DU00-W-350 are 0.5832 and 0.5803 respectively. Therefore, the rate of reduction of the maximum power coefficient is -1.59% for the NACA64618 blade profile, while it is -2.08% for the DU00-W-350 blade profile.

This is because of the maximum lift to drag ratio of DU00-W-350 blade profile is lower than that of NACA64618 blade profile as shown in Figure 19. We can take this example: at $Re = 10^7$,the maximum lift to drag ratio for DU00-W-350 blade profile is equal to 138.6 and for NACA64618 blade profile is equal to 181 .

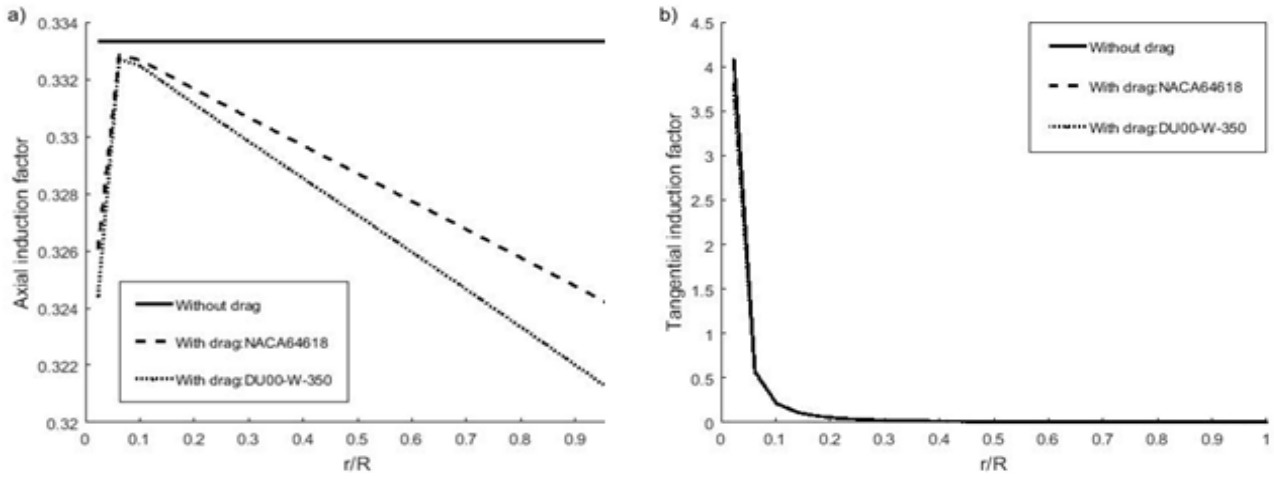

Figure 17: Drag effect on axial and tangential induction factors.

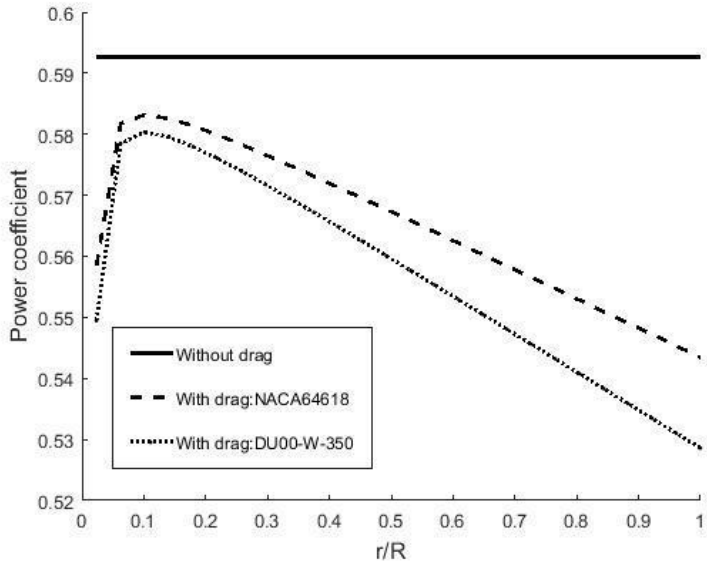

Figure 18: Drag effect on power coefficient.

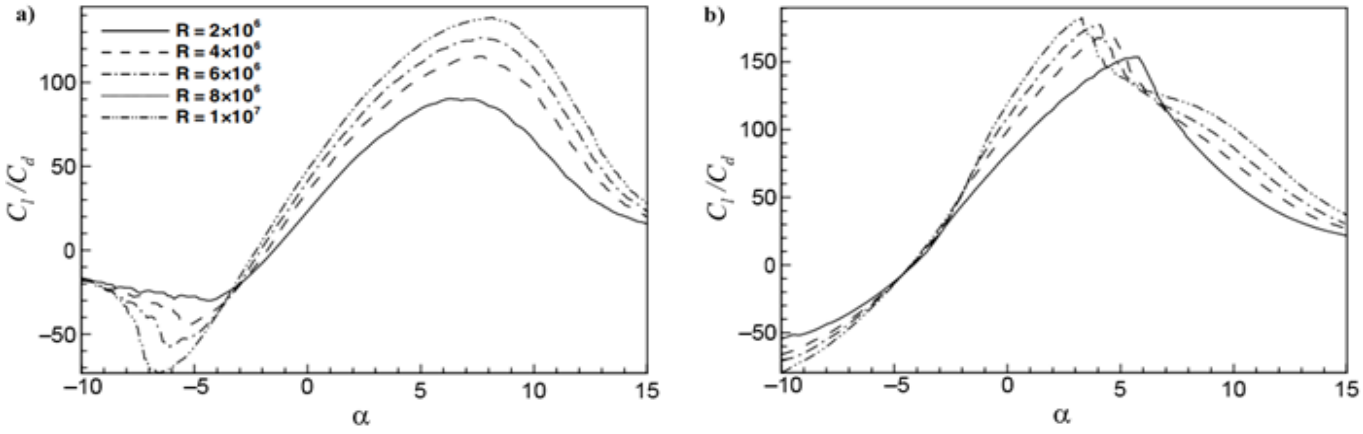

Figure 19: Influence of Reynolds numbers on lift to drag ratio for two airfoils: a) DU00-W-350; b) NACA64618[7].

3.4. Air density effect

To show the effect of air density on aerodynamic performance, the NACA64618 blade profile was selected and two values of air density were used $\rho = 0.820$, $\rho = 1.225$ at a constant specific speed $\lambda = 10$.

The Figure 20 shows that when going from $\rho = 0.820$ to $\rho = 1.225$, the thrust increases from $2433\,N$ to $3636\,N$ near the root positions ($0.1R$) and at the tip of the blade ($1R$) it increases by $1.959 \times 10^4\,N$ to $2.929 \times 10^4\,N$. And the torque increases from $7926\ Nm$ to $1.185 \times 10^4\ Nm$ near the root positions ($0.1R$) and at the tip of the blade ($1R$) it increases from $7.247 \times 10^4\ Nm$ to $1.087 \times 10^5\ Nm$. For the power coefficient, it increases from 0.5826 to 0.583 near the root positions($0.1R$) and at the tip of the blade($1R$), it increases from 0.5403 to 0.5426

(Figure 21). Consequently, it is clear that the increase in thrust and torque and the power coefficient can be strongly dependent on the increase in air density, with an increasing rate of change from root to blade tip. We note that the increase in power coefficient is small compared to the increase in thrust and torque.

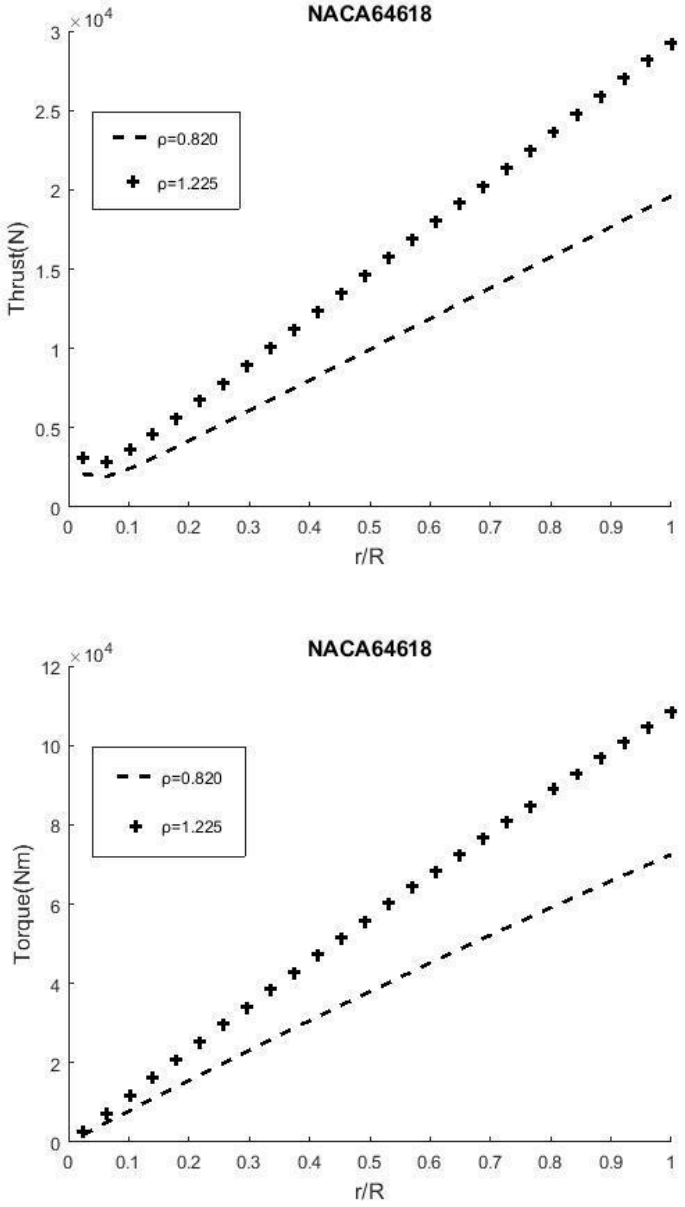

Figure 20: Air density effect on thrust and torque distributions.

This increase in aerodynamic performance can be explained by the fact that the change in air density is strongly correlated with the change in Reynolds number. A change in Reynolds number also affects the maximum ratio of lift to drag C_l/C_d and thus the aerodynamic performance. Hence, a higher air density is better than a lower air density.

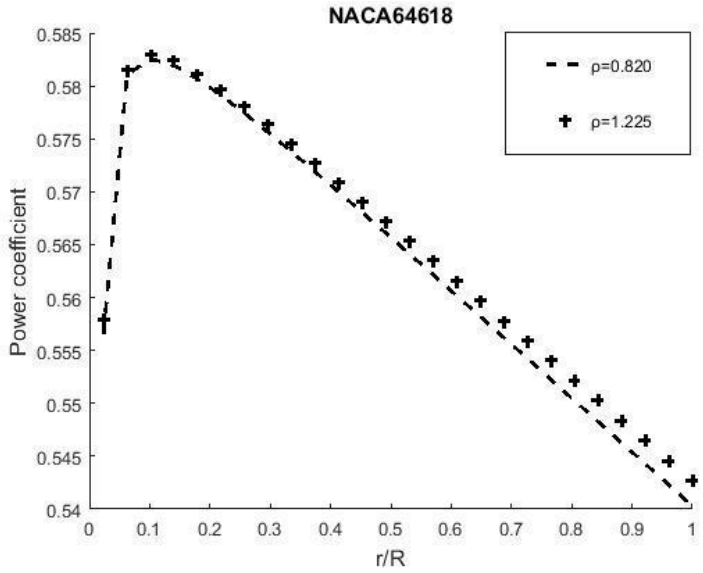

Figure 21: Air density effect on power coefficient.

4. Conclusion

The effect of Reynolds number Re is studied for the DU00-W-350 blade profile though three values: $Re = 2 \times 10^6$, $Re = 6 \times 10^6$, $Re = 10^7$. The effect of drag is examined using a comparison between the blade without drag and the blade with drag for the DU00-W-350 and NACA64618 profiles. The effect of air density for the NACA64618 blade profile is also studied. The simulation is compared with previous work in the literature. The conclusions are:

1) The Reynolds number plays a very important role in improving the aerodynamic performance where an increase in the Reynolds number leads directly to an increase in the torque and power coefficient.

2) The drag has a considerable influence on the aerodynamic performance, i.e. an aerodynamic profile with a low drag coefficient gives a higher torque and power coefficient than an aerodynamic profile with a high drag coefficient.

3) An increase in torque and power coefficient can also be achieved by increasing the air density.

4) The results of the preset work agree well with the result of previous work for all blade positions. However, the differences are observed near the root positions.

Nomenclature

a : Axial induction factor

a' : Tangential induction factor

c : Chord length

N : Number of blades

C_l : Lift coefficient

C_d : Drag coefficient

V_{rel} : Relative wind speed

V_0 : Wind velocity

ϕ : Inflow angle

θ : Pitch angle

α : Angle of attack

Re : Reynolds number

r : Local radius

Ω : Angular velocity of rotor

R : Radius of rotor

ρ : Air density

λ : Tip speed ratio

dT : Aerodynamic thrust

dM : Aerodynamic torque

References

[1] W. Xudong, W. Z. Shen, W. J. Zhu, and C. Jin, "Shape Optimization of Wind Turbine Blades," *Wind Energy*, vol. 12, no. 8, pp. 781–803, 2009.

[2] J. Johansen, H. A. Madsen, M. Gaunaa, and C. Bak, "Design of a Wind Turbine Rotor for Maximum Aerodynamic Efficiency," *Wind Energy*, vol. 12, pp. 261–273, 2009.

[3] E. Benini and A. Toffolo, "Optimal Design of Horizontal-Axis Wind Turbines Using Blade-Element Theory and Evolutionary Computation," *J. Sol. Energy Eng.*, vol. 124, no. 4, pp. 357–363, 2002.

[4] P. Fuglsang and H. A. Madsen, "Optimization method for wind turbine rotors," *J. Wind Eng. Ind. Aerodyn.*, vol. 80, pp. 191–206, 1999.

[5] J. Jonkman, S. Butterfield, W. Musial, and G. Scott, "Definition of a 5-MW Reference Wind Turbine for Offshore System Development," *Natl. Renew. Energy Lab*, no. NREL/TP-500-38060, 2009.

[6] G. Marsh, "Offshore reliability," *Renew. Energy Focus*, vol. 13, no. 3, pp. 62–65, 2012.

[7] M. Ge, D. Ph, D. Tian, D. Ph, and Y. Deng, "Reynolds Number Effect on the Optimization of a Wind Turbine Blade for Maximum Aerodynamic Efficiency," *J. Energy Eng.*, 2014.

[8] M. Drela, "XFOIL: An Analysis and Design System for Low Reynolds Number Airfoils," *Low Reynolds Number Aerodyn.*, pp. 1–12, 1989.

[9] C. Bak, "Sensitivity of Key Parameters in Aerodynamic Wind Turbine Rotor Design on Power and Energy Performance," *J. Phys. Conf. Ser.*, vol. 75, 2007.

[10] W. A. Timmer and R. P. J. O. M. van Rooij, "Summary of the Delft University Wind Turbine Dedicated Airfoils," *J. Sol. Energy Eng.*, vol. 125, pp. 488–496, 2003.

[11] O. Ceyhan, "Towards 20MW Wind Turbine : High Reynolds Number Effect on Rotor Design," *50th AIAA ASM Conf. Nashville, Tennessee*, 2012.

[12] O. De Vries, "On the theory of the horizontal-axis wind turbine," *Annu. Rev. Fluid Mech.*, vol. 15, no. 1, pp. 77–96, 1983.

[13] P. J. Moriarty, "AeroDyn Theory Manual," *Natl. Renew. Energy Lab*, no. NREL/TP-500-36881, 2005.

[14] T. Burton, N. Jenkins, D. Sharpe, and E. Bossayni, *Wind Energy Handbook*, Second Edi. Chichester, England: John Wiley & Sons, Ltd, 2011.

[15] J. G. M. J.F.Manwell, *Wind Energy Explaind ,Theory, Design and Application*, Second Edi. Chichester, United Kingdom: John Wiley & Sons, Ltd, 2010.